Can summer wildfire smoke reduce peak water temperatures in the Salmon River, potentially benefiting cold-water fishes? A preliminary analysis

By:
Aaron T. David
US Fish and Wildlife Service
Arcata, CA

J. Eli Asarian
Riverbend Sciences
Eureka, CA

Frank K. Lake
U.S Forest Service, Pacific Southwest Research Station
Orleans, CA

September 2017

Prepared for the:
Klamath Tribal Water Quality Consortium

Abstract:
We evaluated whether wildfire smoke can cool river water temperatures by attenuating solar radiation and air temperature in the Salmon River, a temperate, Mediterranean ecosystem in Northern California. Previous studies of the thermal effects of wildfires on rivers have focused on either the effect of the heat of combustion on water temperatures during a fire, or the effect of riparian vegetation losses on post-fire water temperatures. We know of no studies of the effects of wildfire smoke on water temperatures of nearby river systems.

We assembled daily data on wildfires, smoke, weather, river discharge, and river temperatures for a 19 year period (1997-2015). Wildfire smoke is difficult to quantify due to high spatial and temporal variability, but we successfully used a newly available daily high-resolution (1-km) dataset of aerosol optical thickness (AOT) derived from satellite imagery to represent smoke density. Solar radiation data from Salmon River stations have data quality issues, so we conducted our evaluation of the effects of smoke on solar radiation using data from the U.S. Climate Reference Network station in Redding, which showed that on the smokiest days at that station, solar radiation was reduced to less than 50% of clear-sky potential. We used linear mixed-effects models to evaluate the effect of wildfire smoke and other variables on daily mean and maximum Salmon River water temperatures in the months June through September in years with major wildfires: 2006, 2008, and 2012-2015. In the best-fitting regression models, air temperature ranks as the strongest predictor, followed by AOT and then discharge. AOT had a greater effect on daily maximum temperatures than on daily mean temperatures. For example, an AOT value of 1700 (nearly the highest three-day average observed) is predicted to decrease maximum water temperature by 1.6°C but decreases mean water temperature by only 0.8°C. Our preliminary results confirm that wildfire smoke reduces solar radiation and water temperatures, but our methods almost certainly underestimate the magnitude of the cooling effect of smoke on water temperatures because air temperatures can also be cooled by smoke and thus is a synergistic effect attributed to air temperature in our models. For example, June 2008 was both the smokiest period of entire study and had the coolest observed stream temperature deviations (up to 4 °C lower than average), yet our model predicted temperatures only 1 °C lower than average. Smoke effects on river temperatures appear to be particularly strong when atmospheric high pressure strengthened inversions trap smoke in river canyons for multi-day periods. This smoke-induced river cooling likely benefits salmonids and other cold-water adapted species during otherwise clear-sky hotter summer temperature periods.

This analysis is a proof of concept to explore methods for analysis and provide an interim deliverable to fulfill contractual obligations. In an upcoming second phase of the project, we will refine our methods using alternative models and datasets, replicate the analysis at many additional sites within the Klamath Basin, and write a manuscript for submission to a peer-reviewed journal.

Suggested citation:
David, A.T., J.E. Asarian, and F.K. Lake. 2017. Can summer wildfire smoke reduce peak water temperatures in the Salmon River, potentially benefiting cold-water fishes? A preliminary analysis. Prepared for the Klamath Tribal Water Quality Consortium by Riverbend Sciences with assistance from the U.S. Fish and Wildlife Service Arcata Office and the U.S. Forest Service Pacific Southwest Research Station. 27p.

Introduction

Temperature is a fundamental regulator of river ecosystems due to the high thermal conductance of water (Beitinger & Fitzpatrick, 1979) and because many aquatic animals are ectothermic, such as fishes, amphibians, and invertebrates (Beschta *et al*., 1987; Gillooly *et al.,* 2002; Neuheimer & Taggart, 2007).

We evaluated whether wildfire smoke can reduce river water temperatures during the season of peak temperatures within the Salmon River of northern California, a temperate, Mediterranean watershed. While wildfire is a distinctly terrestrial phenomenon, fires can substantially affect aquatic ecosystems (Minshall *et al.*, 1989; Gresswell, 1999; Rieman *et al.*, 2012). Wildfires can alter hydrology, sediment dynamics, woody debris, and food webs (Rieman, Gresswell & Rinne, 2012). Wildfires can also impair water quality, including short-term pulses of heavy metals in storm runoff following high-severity fires (Smith *et al.*, 2011; Robinson, 2013, 2014). Several studies have explored the effects of wildfire on lotic water temperatures. Most of these assessments have focused on the effect of the heat of combustion on water temperatures during a fire and the effect of the loss of riparian vegetation on post-fire water temperatures (Hitt, 2003; Dunham *et al.,* 2007; Isaak *et al.,* 2009; Mahlum *et al.,* 2011; Beakes *et al.,* 2014). In contrast, to our knowledge, there are no published studies of the effects of wildfire smoke on the water temperatures of nearby streams and rivers, potentially due to the challenges of sampling during wildfires and the unpredictable and ephemeral nature of wildfires. One regional study found that wildfire smoke inversion in river canyons affected fire behavior and reduced severity (Estes et al. 2017). However, indirect evidence suggests that wildfire smoke has the potential to cool river water temperatures. Wildfire smoke particles absorb and scatter incoming solar radiation (Robock, 1988, 1991; Stone *et al*., 2011), reducing the amount of solar radiation that reaches the Earth's surface (Yu et al. 2016), and can consequently reduce air temperatures (Robock, 1988, 1991; Grell *et al*., 2011; Stone *et al.,* 2011). Mahlum et al. (2011) found that despite reductions in riparian canopy, stream temperatures did not increase during an Idaho fire and speculated that smoke may have reduced solar radiation. Because solar radiation and air temperature are important drivers of stream and river water temperatures (Beschta *et al.,* 1987; Johnson, 2004; Caissie, 2006), we propose that wildfire smoke can reduce river water temperatures via reflectance and absorption of solar radiation and associated reductions in air temperature. The phenomenon is an understudied aspect of wildland fire-fisheries-riverine research.

Specifically, we examined whether wildfire smoke can cool river water temperatures and evaluated the magnitude of the effect of smoke on water temperatures relative to other variables known to influence lotic water temperatures. To address these questions we assembled data on water temperature, wildfire smoke, weather, and river discharge from a 19 year period (1997-2015) in a large watershed in Northern California. If wildfire smoke does reduce lotic water temperatures, this phenomenon may suggest that historical pre-suppression fire regimes with more frequent return intervals may have attenuated maximum summer water temperatures in some watersheds, potentially benefiting salmonids and other cold water-adapted species.

This analysis is a proof of concept to explore methods for analysis and provide an interim deliverable to fulfill contractual obligations. In an upcoming second phase of the project, we will replicate the analysis at many additional sites within the Klamath Basin and write a manuscript for submission to a peer-reviewed journal.

Study Area

We conducted our analysis in the Salmon River, located in Siskiyou County, California, USA (Figure 1). The watershed is sparsely populated with only about 250 people residing within the 751 mi^2 watershed, 98.7% of which is managed by the U.S. Forest Service (Elder et al. 2002). The Salmon River was identified as a high priority Key Watershed in the Northwest Forest Plan and it contains some of the best anadromous fisheries habitat in the entire Klamath River basin. Elevations range from 500 feet to 9000 feet (Elder et al. 2002). Much of the watershed is steep, mountainous terrain. Precipitation ranges from less than 40 inches along the South Fork to over 80 inches in upper Wooley Creek (Elder et al. 2002). The Salmon River watershed is located within the Klamath Mountains physiographic province. Approximately 81% of the watershed is covered in conifer forest, with 9% in hardwood forests (Elder et al. 2002).

We focused our analysis on the Salmon River sub-basin for three reasons. First, the forests of the Klamath-Siskiyou Mountains are fire-prone ecosystems that experience fires of a variety of sizes, severities, and frequencies (Taylor & Skinner, 1998, 2003; Halofsky *et al*., 2011, Estes et al. 2017). In addition to lightning ignitions, Native Americans traditionally used fire to manage natural resources in the basin (Lake, 2007, 2013). Like many forested ecosystems in the Western USA, the Klamath-Siskiyou Mountains have been altered by fire suppression and logging, generally resulting in less-frequent fires (Taylor & Skinner, 1998, 2003). Second, anecdotal observations in the basin suggested that river temperatures are reduced during periods of heavy smoke from summer wildfires, stimulating interest by natural resource agencies, Native American tribes, and others responsible for managing Pacific salmon populations within the basin (Lake 2009, SRRC 2014, Karuk Tribe 2014). Third, like many watersheds in northern California, the Salmon River has been substantially impacted by human activities, including logging, mining, and road building (NCRWQCB 2005). Naturally high water temperatures in parts of the basin have been exacerbated by post-American settlement human modifications to the landscape, resulting in negative impacts to salmon populations. The river is listed as impaired by high water temperatures under the federal Clean Water Act, and the State of California has developed a Total Maximum Daily Load (TMDL) for water temperature (NCRWQCB 2005).

Methods

We confined all data and analyses to June 1 through September 30 of each year because this is the season when water temperatures are typically the highest and most likely to be stressful to cold-water adapted species in the region and when wildfires are most likely to be actively burning and producing smoke.

Water Temperature Data

We assembled water temperature records for the Salmon River at Somes Bar near the confluence with the Klamath River (Figure 1) collected between 1997 and 2015. These temperature data were collected by the U.S. Forest Service. Water temperatures were measured using digital data loggers and standard protocols (Dunham *et al.,* 2005).Temperature monitoring did not always encompass the entire June 1 to September 30 period. If the start and end dates of monitoring fell between June 1 and September 30, we removed the start and end dates when less than 75% of the day was sampled. Because of the long record, the type of logger used and the measurement frequency often changed through time. Measurement frequency ranged from 30 min to 60 min.

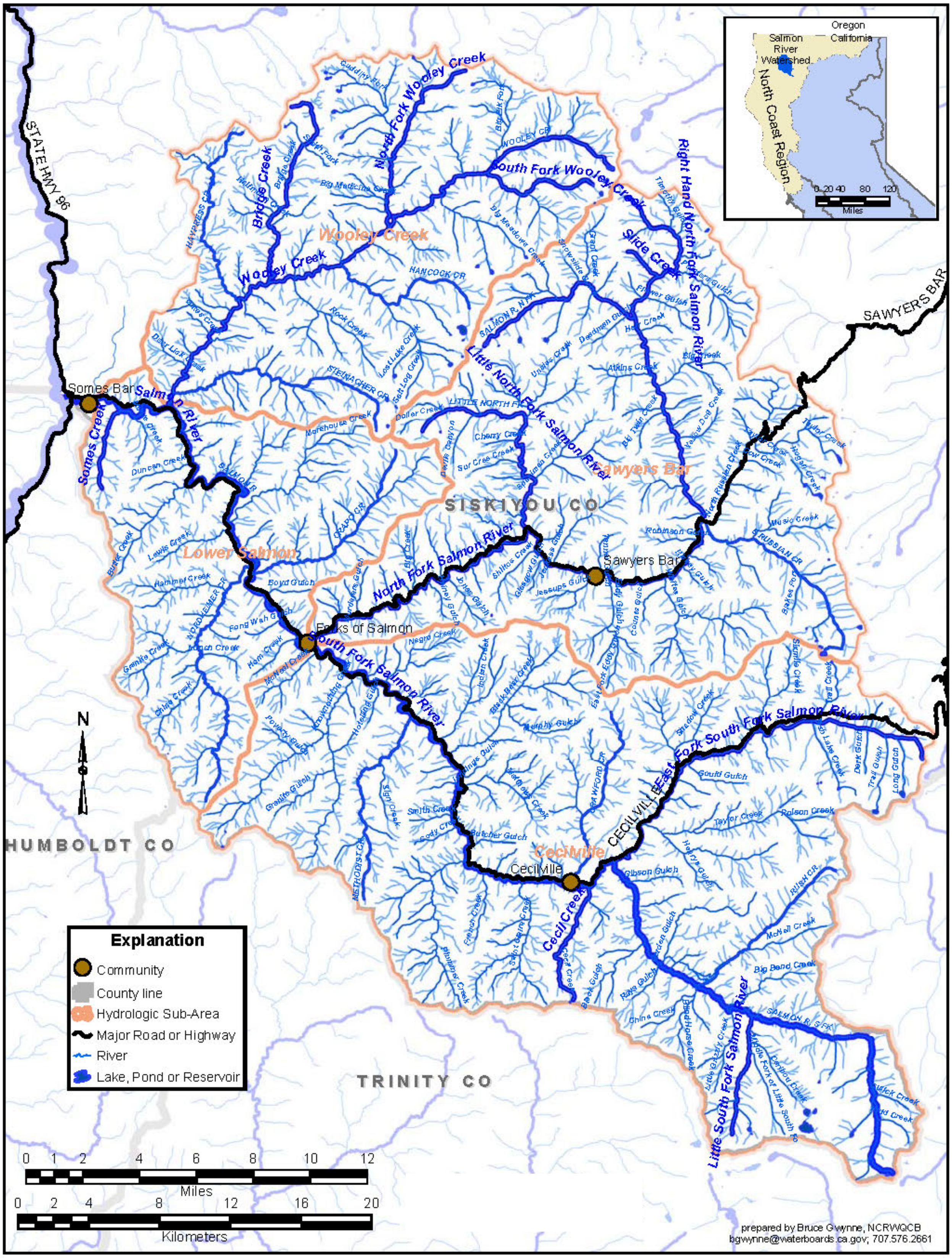

Figure 1. Map of Salmon River sub-basin. Figure copied from NCRWQCB (2005).

We calculated daily means, minimums, and maximums from the raw water temperature data. All temperature time series were visually examined and compared with nearby concurrent temperature time series (when available) to identify suspicious measurements. Suspicious measurements were examined further and removed if determined to be erroneous.

Instead of using the observed temperatures as our response variables in the analyses of wildfire smoke effects on water temperatures, we converted daily mean and maximum water temperatures to deviations from long term averages. We did this for two reasons. First, we wanted to remove the seasonal pattern that water temperatures often exhibit that is not fully captured by variation in air temperature and other meteorological variables (Benyahya *et al.,* 2007). Second, because wildfires and wildfire smoke were not evenly distributed throughout the summer season (see results), we did not want to confound effects of smoke with otherwise normal seasonal variation in water temperatures. For each year, we calculated the long-term average of daily mean and maximum temperatures for each calendar day, excluding data from the current year from the calculation. Because the numbers of years in our time series of water temperatures were modest, we wanted to ensure we were not fitting noise in our calculations of long-term averages. Thus, we fit a locally weighted second-degree polynomial regression to the daily long-term averages for each year as a function of calendar day. The regression used 20% of the data in fitting each point. For each year we subtracted the fitted long-term daily average means and maximums from the observed daily means and maximums. These daily mean and maximum water temperature deviations were the values we used for analysis.

Wildfire Smoke Data

We used imagery from the Moderate Resolution Imaging Spectroradiometer (MODIS) instruments on board the National Aeronautics and Space Administration's (NASA) Terra and Aqua satellites to identify when wildfire smoke was present over the lower Klamath Basin region. Terra and Aqua have sun-synchronous, near polar orbits. Terra passes over Northern California each morning and Aqua each afternoon. Starting with 2004, true-color, geometrically-corrected MODIS subset images were available for nearly every day at a resolution of 250 m^2. Imagery were primarily obtained from NASA's Land, Atmosphere Near real-time Capability for Earth Observing Systems website (LANCE)(https://earthdata.nasa.gov/earth-observation-data/near-real-time). On days when LANCE images were not available, we used similar images from Space Science and Engineering Center at the University of Wisconsin-Madison (http://ge.ssec.wisc.edu/modis-today).

We examined MODIS imagery of Northern California each day between June 1 and September 30, 2004-2015 to determine if wildfire smoke was present over any part of the lower Klamath Basin. Smoke was typically easy to distinguish in imagery (Figure 2d). To confirm we were not misinterpreting the MODIS imagery, we used the spatial database of USA wildfires developed by Short (2014, 2015) to identify when fires were burning in or near the lower Klamath Basin. This database encompasses 1992 through 2013. For 2014 and 2015, we used the Incident Information System (INCI web; http://inciweb.nwcg.gov/) to identify when fires were burning in or near the basin. The Short (2014, 2015) database, INCI web, and our personal observations in the region all indicated that the MODIS imagery accurately captured the occurrence of wildfire smoke in the area of interest. These data sources also indicated that 2006, 2008, and 2012-2015 were moderately to very smoky summers. Thus, all further analyses were conducted using only data from these years.

We also used MODIS data to quantify the distribution and density of wildfire smoke. The measure of smoke we used was aerosol optical thickness (AOT), which is commonly used in air quality studies and measures the degree to which aerosols prevent the transmission of light by absorption or scattering (Duncan et al., 2014; Chu et al., 2016). We used 1 km^2 resolution gridded AOT data derived from multiple MODIS spectral bands processed according to the multi-angle implementation of atmospheric correction algorithm (MAIAC; Lyapustin *et al*., 2011a,b, 2012a,b; Di *et al.*, 2016). These AOT data were available from one to three times per day, depending on the location of satellite overpasses. While the MAIAC algorithm improves upon other AOT retrieval methods, it is unable to retrieve AOT from grid cells where clouds are present (Lyapustin *et al*., 2011a,b, 2012; Superczynski 2017). Thus, the AOT data often contained null values for some grid cells (Figure 2a). We used the Fire INventory from NCAR (FINN; Wiedinmyer *et al.,* 2011) data set along with a spatial interpolation algorithm to infill grid cells with missing AOT values. FINN is a spatially explicit fire occurrence data set derived from MODIS thermal anomaly data with a 1 km^2 spatial resolution and a daily temporal resolution (Wiedinmyer *et al.,* 2011). If an AOT grid cell with a null value contained a FINN fire occurrence for the same day, we assigned that grid cell an AOT of 3000 (75% of the maximum possible value 4000, selected based on visual exploration). Fire occurrences were used to help infill missing AOT values because the MAIAC algorithm can mistake grid cells containing dense smoke as clouds (Lyapustin *et al*., 2012a,b), thus biasing the AOT estimate for a region low. Next we used the Close Gaps with Spline module from the System for Automated Geoscientific Analyses (SAGA, http://www.saga-gis.org), implemented within R (R Core Team, 2015) using the rsaga package (Brenning, 2008), to spatially interpolate the remaining null value grid cells in each satellite pass. The Close Gaps with Spline module uses observed values where present and fills in gaps by fitting spline functions to the observed data. Advantages of this interpolation approach include: 1) it allows interpolated values to be greater than input values, which is necessary given that many null values were due to heavy smoke whereas nearby areas of lighter smoke were not null, 2) all non-missing data values were retained and not altered by the interpolation (Reid et al., 2015). After interpolation, all values greater than 4000 (the maximum possible AOT value) were reduced to 4000. The result was a fully infilled gridded AOT data for each MODIS pass over Northern California (Figure 2c). We also ran the same interpolation algorithm without the FINN data (Figure 2b). For each satellite pass, we visually examined the original gridded AOT data with null values, the FINN-interpolated AOT data, the interpolated AOT data without the FINN fire occurrences, and the corresponding MODIS true color image. We discarded all satellite overpasses when the pass did not fully encompass our focal area. We used the FINN-interpolation version for most overpasses, but substituted non-FINN interpolations when the FINN interpolation performed poorly (103 out of 2994 overpasses), typically due to a combination of smoke and extensive cloud cover. We discarded two overpasses for which neither the FINN nor the non-FINN interpolation produced gridded AOT data that reasonably matched the associated true color MODIS image.

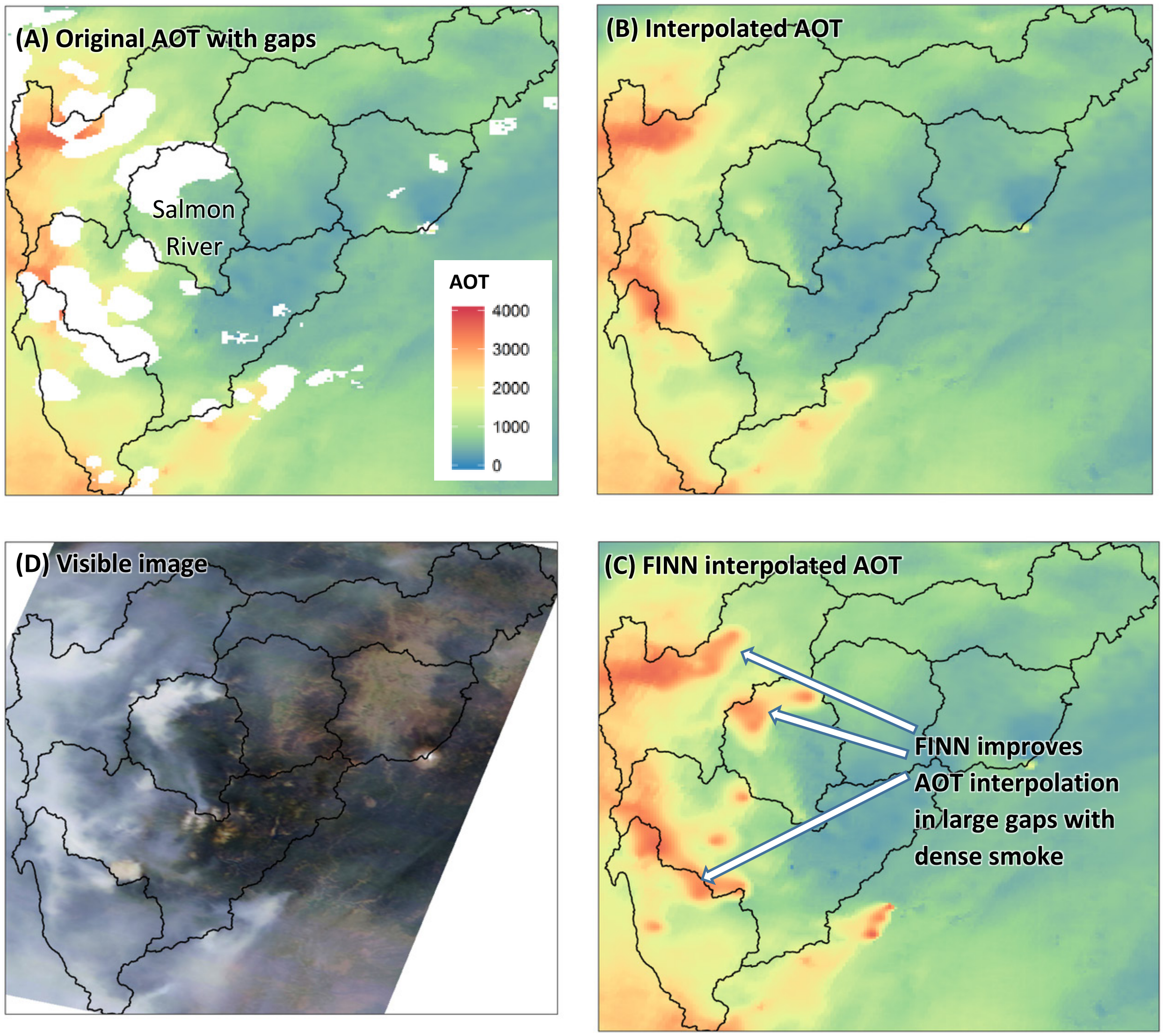

Figure 2. Comparison of (A) original aerosol optical thickness (AOT) before interpolation of gaps due to clouds or dense smoke plumes, (B) AOT interpolated to fill gaps, (C) AOT with fire inventory (FINN) points inserted and then interpolated, and (D) visible MODIS imagery for an example satellite pass (MODIS Terra on July 12, 2008 at 1830 hours, Julian day 194). Black lines are boundaries of sub-basins (level 4 hydrologic units) in the Klamath Basin, with the Salmon River sub-basin labeled in the upper-left panel.

Next, we delineated the watershed upstream from the water temperature monitoring location. We then calculated a mean AOT value for the temperature monitoring watershed area on each day within our period of interest. If there was more than a single pass for each satellite in each day we first calculated the mean AOT value of each satellite within a day, and then calculated the mean AOT value of the two satellites for each day. We noticed that on cloudy, smoke-free days, the interpolation algorithm often appeared to overestimate AOT values. Thus, for all days when we had previously determined there was no smoke present anywhere in the lower Klamath basin using the MODIS true color imagery, we assigned those days the lower quartile of all the daily

AOT values for smoke-free days. Because the Salmon River is situated close to the Pacific Coast in a region of low population density, it is reasonable to assume that wildfire smoke is the only major producer of aerosols in the region. For example, in Siskiyou County for the year 2012, wildfires accounted for 90% of fine (less than 2.5 microns in diameter) particulate matter emissions (CARB 2013). Thus, assigning a uniform low AOT value to all smoke-free days should not bias our analysis. Finally, for 11 days across the six years that were classified as smoky but did not have at least one valid satellite pass (i.e., either there were no data, or we discarded all overpasses after visual examination), we assigned those days the mean of the AOT values from the day before and the day after.

Weather and River Discharge Data

In addition to AOT as a measure of smoke density, we assembled river discharge and meteorological data to evaluate as potential drivers of water temperature variation and to assess the influence of smoke density (AOT) on surface solar radiation. We downloaded mean daily discharges for the Salmon River from the U.S. Geological Survey (http://waterdata.usgs.gov/nwis) for our period. Precipitation data for the watershed area upstream of the temperature monitoring location were acquired from the University of Idaho gridded surface meteorological dataset (Abatzoglou, 2013). This dataset provides a variety of gridded meteorological variables at a daily temporal resolution and a 4 km spatial resolution for the coterminous United States, but we only used precipitation which combines daily data from the North American Land Data Assimilation System Phase 2 (NLDAS-2, Mitchell et al., 2004) with monthly data from the widely used Parameter-Elevation Regressions on Independent Slopes Model (PRISM) dataset (Daly *et al.*, 2008). We used minimum and maximum daily air temperature data from 800 m resolution grids from Topography Weather which are derived from a combination of weather station data (including the Remote Automated Weather System [RAWS] network which is an important data source in the Klamath Basin), elevation-based predictors of temperature, and long-term averages of remotely sensed 1-km land skin temperature (Oyler *et al.*, 2014). The lack of spatial and temporal gaps in the gridded temperature and precipitation datasets makes them much easier to use than individual weather stations, but users should be aware of their limitations (Behnke et al. 2016). For example, the Topography Weather dataset has known biases in foggy areas of the California coast (Oyler *et al.*, 2014), but our study site is far enough inland that it should not be affected. We calculated mean minimum and maximum air temperatures and accumulated precipitation for the watershed across each day using the USGS geo data portal (https://cida.usgs.gov/gdp/). Subsequently, we calculated mean daily air temperatures from the minimum and maximum air temperatures.

Solar Radiation Data

The solar radiation data from the RAWS stations have some data quality issues[1] that make it difficult to extract a clean, reliable time series. Therefore, we used the Redding, California station of the U.S. Climate Reference Network (USCRN), which has extremely high data quality data, to quantify the effect of wildfire smoke on solar radiation in Northern California. Hourly solar radiation data were available starting in 2003. For each day we calculated the mean solar radiation (W/m^2) between 09:00 and 17:00. For each calendar day, we identified the maximum

[1]Data quality issues included apparently erroneous spikes, shifts in calibration (i.e., differences in unobstructed insolation among years), and data gaps.

value of mean solar radiation across 2003 – 2015. We assumed this maximum value represented completely clear sky conditions (i.e., no clouds or smoke). For the six moderate to heavy smoke years, we than calculated the ratio of the observed mean solar radiation on each day to the maximum solar radiation value for the same calendar day. The resulting values represent the observed solar radiation as a ratio of the expected solar radiation under totally clear sky conditions for the same day of the year. Using the process described above in the *Wildfire smoke* section, we also calculated mean daily AOT values for a 10 km – radius circle around the Redding USCRN station for the six years. These solar radiation data were not used in the water temperature analysis, but rather only used for evaluating the effect of smoke on solar radiation.

Solar Radiation Analysis
To evaluate the effect of wildfire smoke on solar radiation, we regressed the Redding AOT data against the Redding solar radiation data (observed radiation as a fraction of clear radiation) for each June-October day in our six-year study period.

Water Temperature Analysis
We used linear regression to evaluate the effect of wildfire smoke (daily mean AOT) on daily ratios of observed solar radiation to expected solar radiation given clear-sky conditions at the Redding USCRN station. Prior to performing the regression, we excluded all cloudy days as determined by examining MODIS true color imagery to allow us to isolate the effects of smoke. If imagery from either satellite contained clouds over or near the USCRN station, we dropped that day from the analysis. While these data constitute a time series, we did not incorporate any temporal correlation structure in the regression. In the absence of external forcing (e.g., smoke, clouds), daily solar radiation varies in a predictable manner and there should not be any lagged effects, precluding the need to account for the temporal structure of these data.

We used linear mixed-effects models fit via maximum likelihood to evaluate the effect of wildfire smoke and other variables on daily mean and maximum water temperature deviations. Models were fit separately for the two response variables. A random intercept of year was included in the models because water temperatures can vary overall year to year. Within each year we incorporated a first-order autoregressive correlation structure to account for the temporal nature of the data and the strong thermal inertia of water. We first fit a full model that included wildfire smoke (AOT), air temperature, precipitation, river discharge, and an interaction between air temperature and river discharge as explanatory variables. Specifically, we used three day trailing averages of AOT, air temperature, precipitation, and daily values of river discharge. The interaction term was included because we expected that the effect of air temperature would increase as discharge decreased (Webb *et al.,* 2003). If any of the explanatory variables had a P value > 0.05, we dropped the variable with the largest P value, refit the model, and then compared the two models with a likelihood ratio test using the same criterion ($P > 0.05$). This backwards-selection process was repeated until all remaining variables in the model had a P value ≤ 0.05. All analyses were performed using the R software for statistical computing (R Core Team, 2015). The linear mixed-effects models were implemented using the nlme package (Pinheiro *et al.,* 2017).

Results

Effect of Wildfire Smoke on Solar Radiation

There was a significant relationship between AOT and solar radiation measured at the USCRN station near Redding on cloud-free days in 2006, 2008, and 2012-2015 ($r^2 = 0.74$, $p < 0.001$; $\beta = -0.0001571$) (Figure 3). On the single smokiest day, solar radiation was reduced to less the 50% of clear-sky potential, while on moderate and heavy smoke days (i.e., AOT>500) solar radiation was reduced to 60-95% of clear-sky potential.

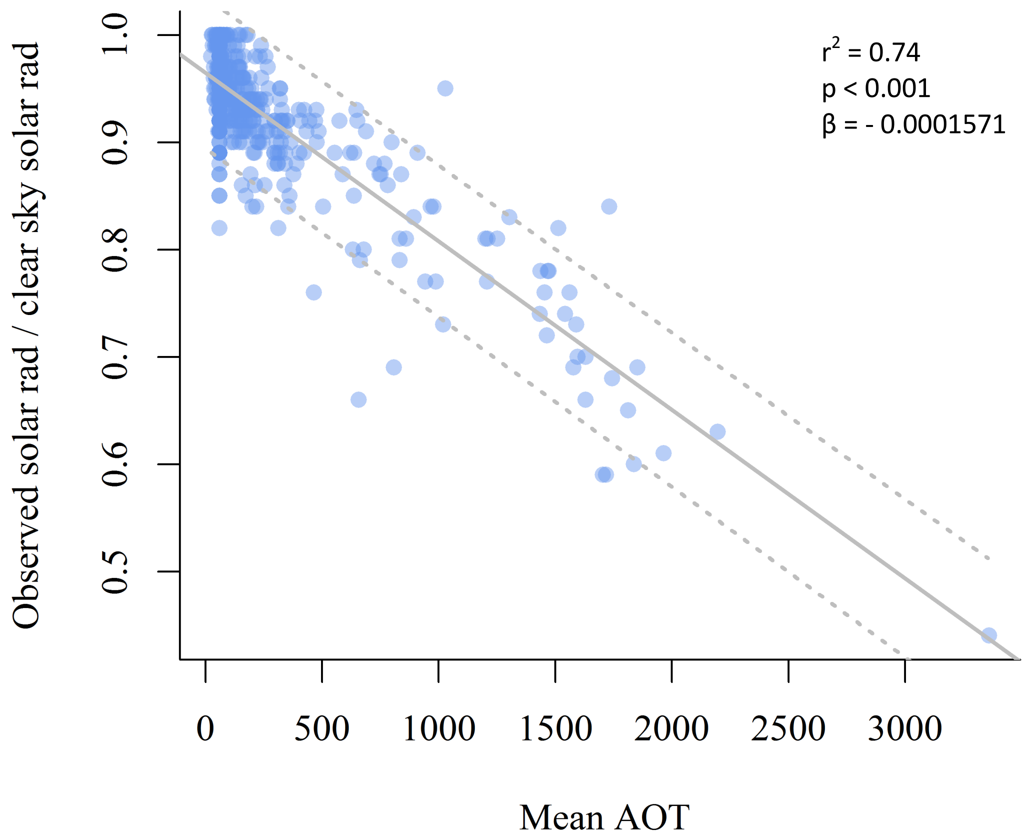

Figure 3. Remotely sensed wildfire smoke (mean aerosol optical thickness, AOT) vs. solar radiation measured at the U.S. Climate Reference Network station near Redding on cloud-free days in 2006, 2008, and 2012-2015. Solid line is regression line and dotted lines are 95% confidence intervals for the prediction of new solar radiation values. r^2 = coefficient of determination, with the value of 0.74 indicating that AOT explains approximately 74% of the variance in solar radiation; p-value = probability that solar radiation is not associated with changes in AOT, with the low p-value indicating a very high probability that the two variables are related; and β = regression slope (change in radiation per unit change in AOT).

Effect of Wildfire Smoke on River Temperatures
Scatterplots of the deviation of maximum water temperature and predictor variables indicates that (Figure 4a) water temperatures tend to be cooler as smoke increases and tend to be warmer as air temperatures increase. Water temperatures also are cooler when precipitation and discharge are high, although the relationships are weaker and only apparent at high values. The same plot of the deviation of mean water temperature and predictor variables shows similar relationships (Figure 4b).

In the best-fitting regression models, air temperature ranks as the strongest predictor, followed by AOT and then discharge (Table 1). Precipitation was only significant in the mean temperature model (Table 1). The coefficient (i.e., change in water temperature per unit change in the variable) for AOT was nearly twice as high for the daily maximum model (0.000934 °C/AOT) as the daily mean model (0.000479 °C/AOT) (Table 1). For example, an AOT value of 1700 (nearly the highest three-day average observed) is predicted to decrease maximum water temperature by 1.6°C but decreases mean water temperature by only 0.8°C.

The regression models predict a lower range (i.e., deviations closer to zero) of maximum and mean temperatures than was actually observed, with high values underestimated and low values overestimated (Figures 5, 6, and 7).

As a simple alternate method for evaluating of the effect of smoke, within each year we calculated the mean water temp deviation for days with a three-day mean AOT < 100 (clear or very low smoke) and for days with a three-day mean AOT >= 500 (at least moderate smoky). Excluding the two years with only a few days of clear or very low smoke (2008) or at least moderate smoke (2012), the moderately smoky days were on average 1.37 to 3 °C cooler than the clear or very low smoke days (Table 2).

Table 1. Comparison of parameter estimates for models to predict deviation of daily maximum and mean water temperatures. Variables are listed in order of importance (i.e., absolute value of t statistic). Coefficient = change in water temperature per unit change in the variable; Standard Error = standard error of coefficient (i.e., uncertainty in estimate of coefficient); p-value = probability that the coefficient is equal to zero (i.e., no effect), with lower p-values indicating greater degree of statistical significance; t-value = coefficient divided by standard error. The greater the absolute value (i.e., how far it is from zero in either a positive or negative direction) of the t-value, the less uncertain in the coefficient and the greater the influence of the variable on the predicted water temperatures.

Model	**Variable**	**Coefficient**	**Standard Error**	**Degrees Freedom**	**t-value**	**p-value**
Daily maximum temperature, with autocorrelation and random effect for year						
	Intercept	-2.88	0.56	577	-5.18	<0.001
	Air temperature 3-day avg.	0.180	0.016	577	11.46	<0.001
	AOT 3-day avg.	-0.000934	0.000157	577	-5.95	<0.001
	Discharge daily	-0.000470	0.000196	577	-2.39	0.017
	Precipitation 3-day avg.	-0.486	0.223	577	-2.18	0.030
Daily mean temperature, with autocorrelation and random effect for year						
	Intercept	-3.11	0.54	578	-5.80	<0.001
	Air temperature 3-day avg.	0.190	0.010	578	18.59	<0.001
	AOT 3-day avg.	-0.000479	0.000104	578	-4.62	<0.001
	Discharge daily	-0.000408	0.000123	578	-3.32	0.001

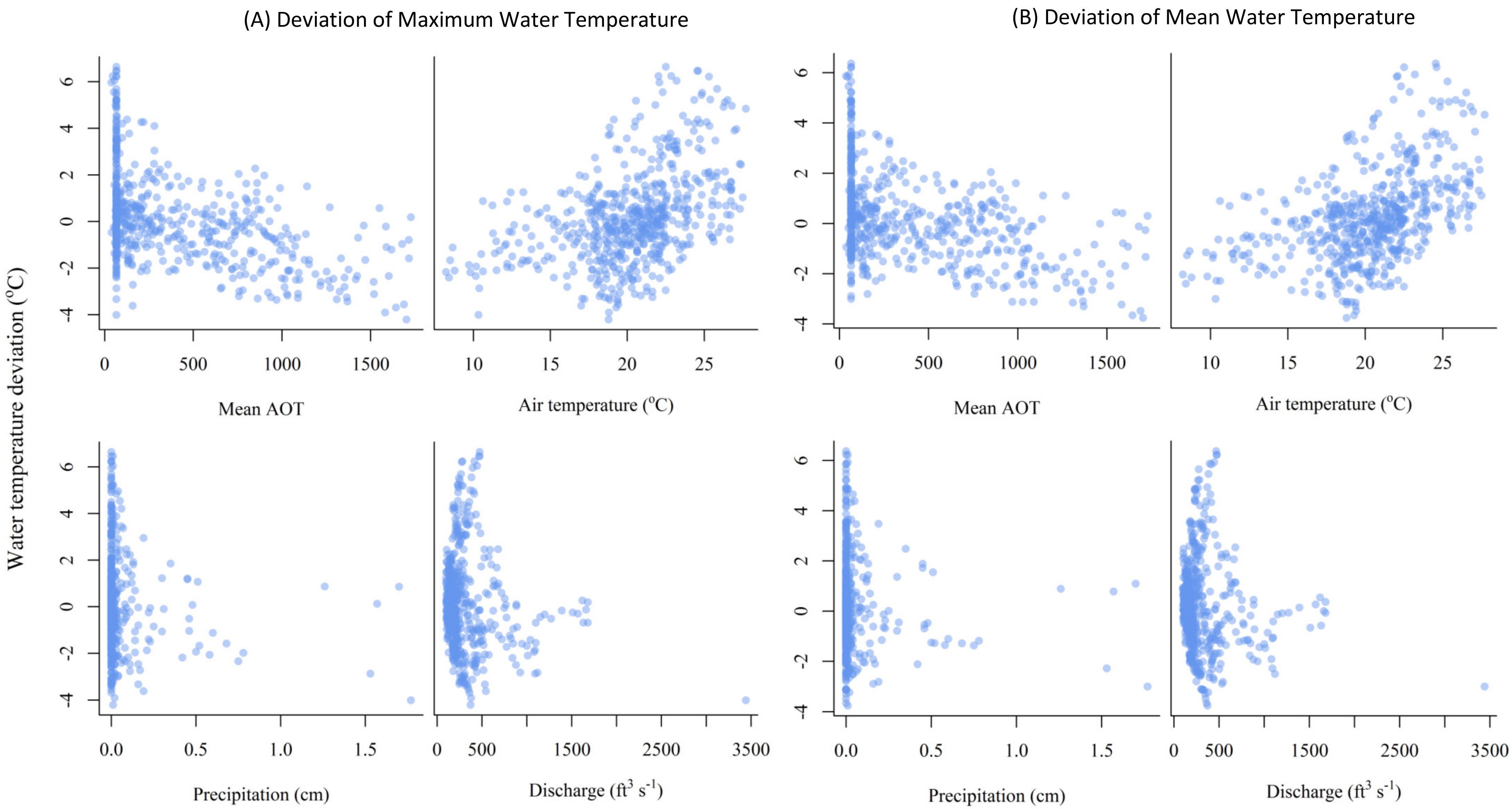

Figure 4. Relationships between four predictor variables (remotely sensed wildfire smoke [mean aerosol optical thickness, AOT], air temperature, precipitation, and discharge) and (A) deviation of maximum water temperature and (B) deviation of mean water temperature. Discharge is daily values while AOT, air temperature, and precipitation are three day trailing averages.

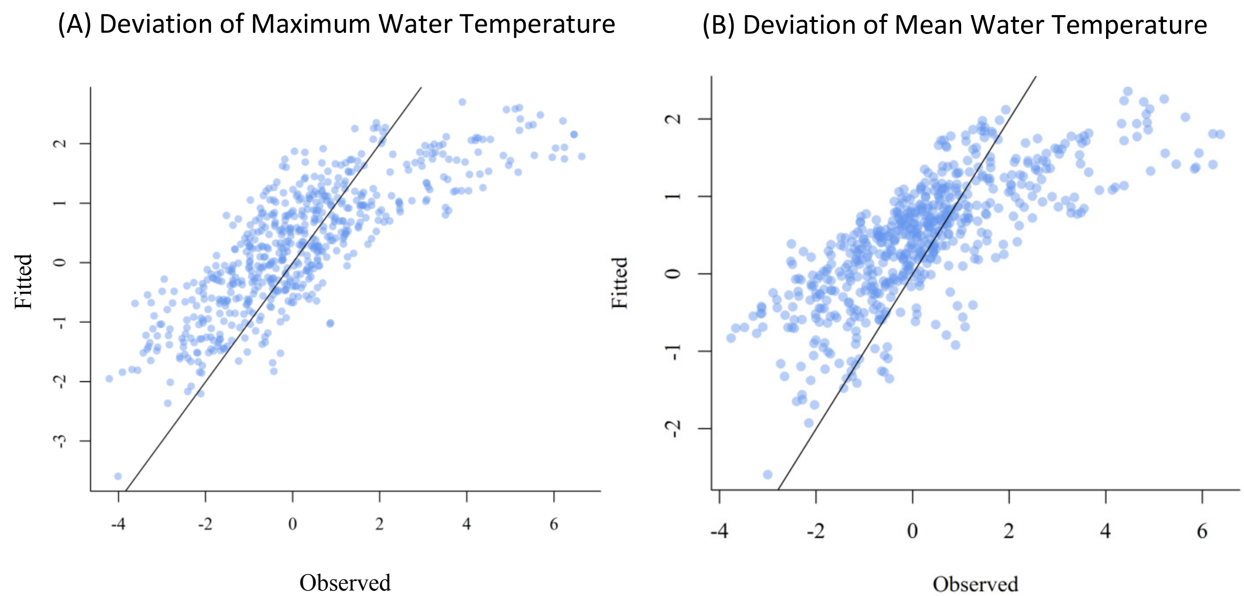

Figure 5. Modeled vs. observed deviations of (A) maximum daily water temperature, and (B) mean daily water temperature. The solid line is the Y=X identity line.

Table 2. Mean water temp deviation for days with a three-day mean AOT < 100 (clear or very low smoke) and for days with a three-day mean AOT >= 500 (at least moderately smoky). See below.

Year	<100	>=500	Diff
2006	-0.21	-1.58	-1.37
2008	-0.40*	-2.05	-1.65*
2012	-0.36	1.13*	1.49*
2013	0.66	-1.26	-1.92
2014	2.37	0.78	-1.59
2015	2.81	-0.19	-3.00

*Note: 2012 only had two days with >= 500 AOT and 2008 only had four days with AOT < 100, so the comparison is less reliable for those years.

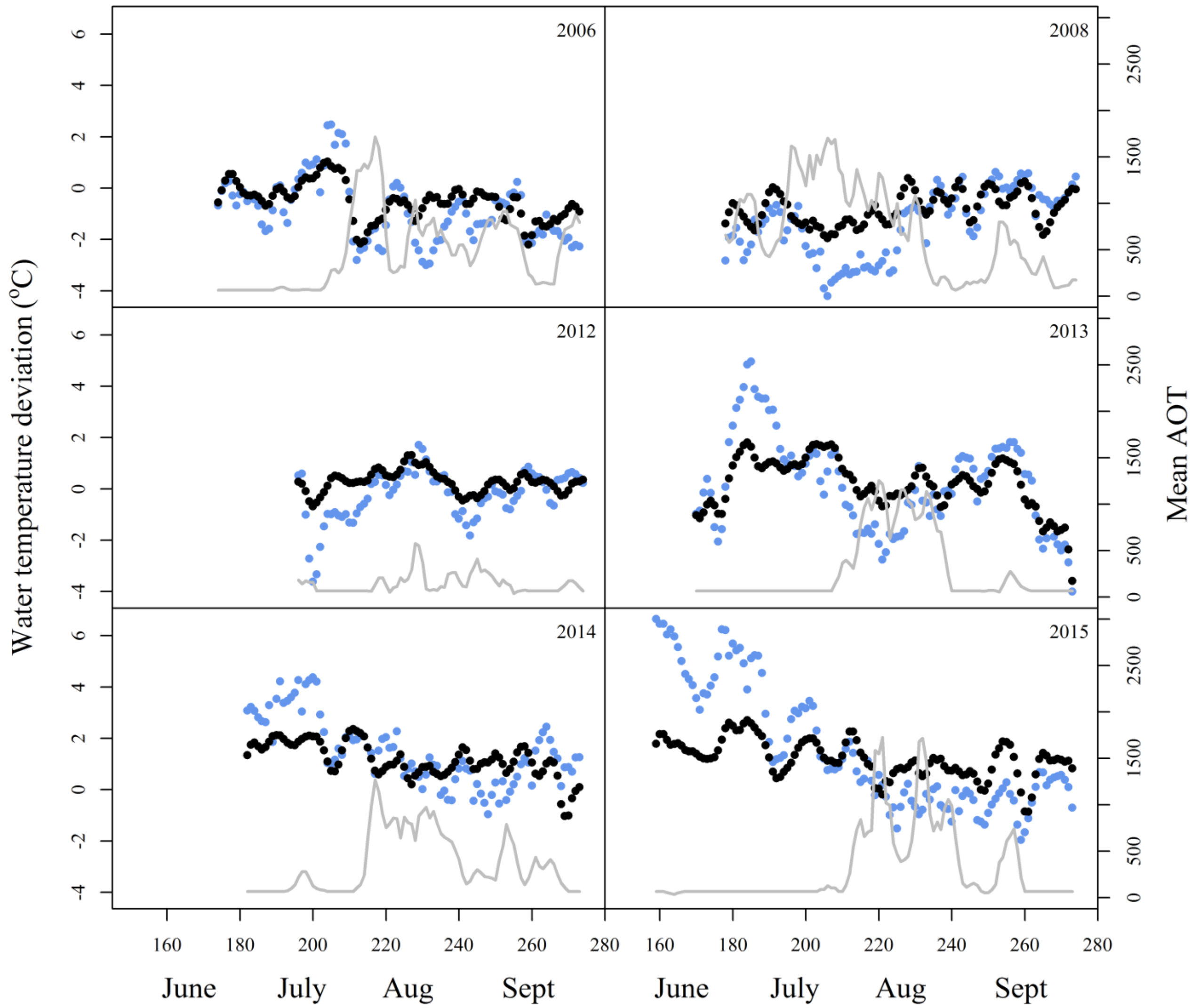

Figure 6. Daily time series for each year showing AOT and deviation of maximum water temperature. Blue points are observed water temps, black points are fitted (modeled) water temps, and the gray line is the three-day trailing AOT average for the basin.

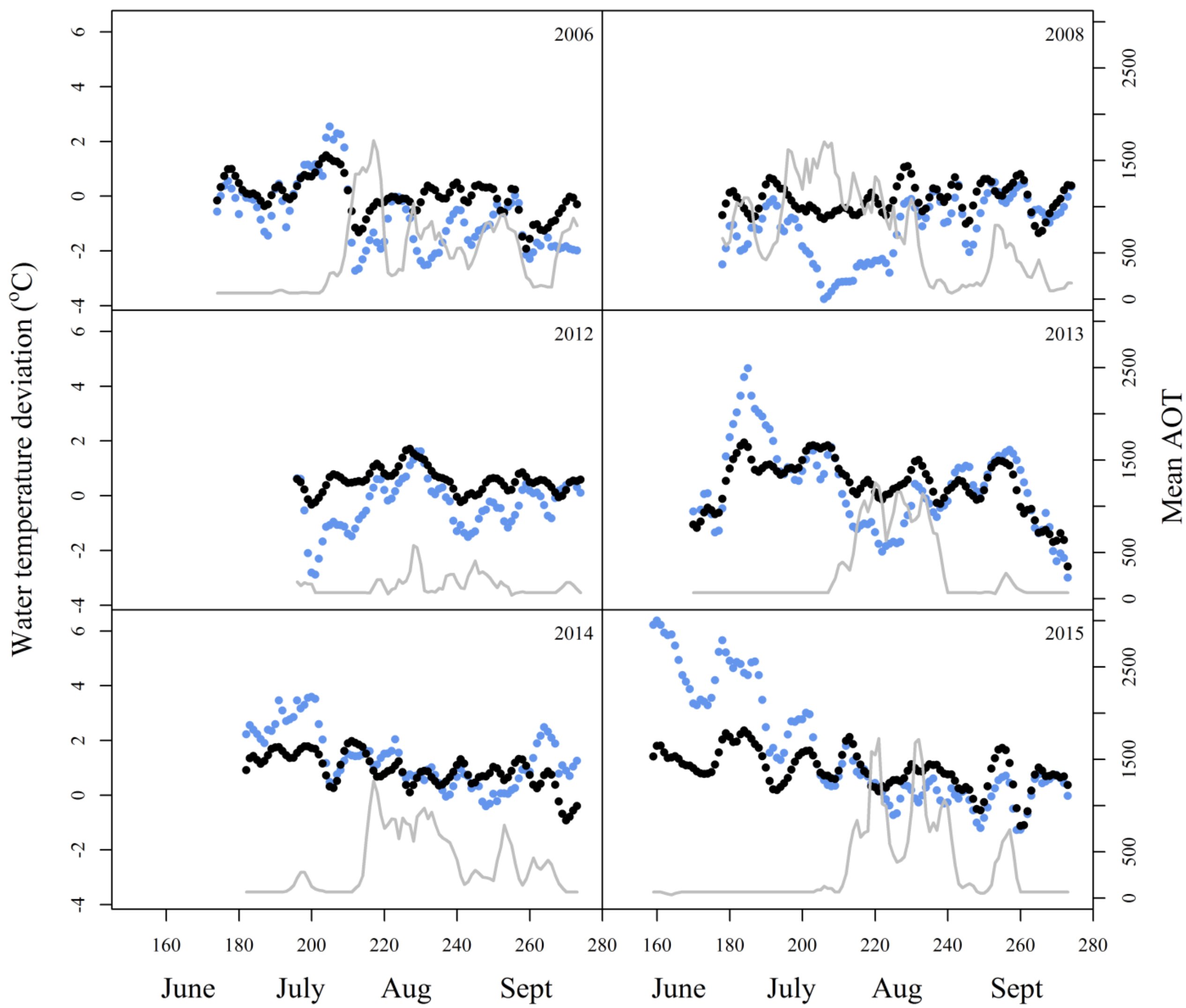

Figure 7. Daily time series for each year showing AOT and deviation of mean water temperature. Blue points are observed water temps, black points are fitted (modeled) water temps, and the gray line is the three-day trailing AOT average for the basin.

Discussion

Our results confirm that wildfire smoke reduces solar radiation and river water temperatures. Smoke may be a particularly important during droughts when streams are more prone to heating. Given that wildfires are expected to increase as the climate warms (Westerling et al. 2008, 2011; Gergel et al. 2017), smoke may be a mechanism for climate change resiliency. Prescribed fire and managed wildfire could be valuable tools for managing stream temperatures in coldwater fish habitat. A reduced emphasis on fire suppression and return towards a more natural fire regime with more frequent return intervals should provide benefits to salmonids and other cold water-adapted species. We recognize the significant challenges and risks of allowing fire to return to the landscape, but our results suggest that fire provides an additional potential benefit that has not yet received appropriate recognition in the scientific literature even though it is well known to local people within our study area (see Bisson et al., 2003,O'Laughlin, 2005).

Similar to results from many previous studies (Mohseni et al., 1998; Mayer, 2012; Luce et al., 2014), we found a strong correlation between air temperature and water temperature; however, this correlation does not imply causation (Johnson, 2003; Caissie, 2006). Air temperature and water temperature are highly correlated because both respond to the same temporal patterns in solar heating (Johnson, 2004). Incoming solar radiation is the most important term in stream energy budgets (Johnson, 2003). In contrast, convection of heat from air to water is much less important process (Johnson, 2004). Previous research on the Klamath River in summers 2004 and 2005 found that adult salmon migration was triggered by a 2°C reduction in river water temperature preceded by reductions in solar radiation and air temperature during large-scale weather fronts with clouds (Strange, 2010).

Our methods almost certainly underestimate the magnitude of the effect of smoke on water temperatures. For example, June 2008 was both the smokiest period of entire study and had the coolest observed temperature deviations (up to 4 °C lower than average), yet our model predicted temperatures only 1 °C lower than average (Figures 5 and 6). Air temperature was the strongest predictor of water temperature in our regression model (Table 1), but air temperatures are also cooled by the smoke (Turco 1990). We experimented with ways to statistically account for the effect of smoke on air temperature but have not yet been successful due to the multitude of factors that affect air temperature (e.g., day length, atmospheric circulation patterns, clouds, etc.). We also experimented with using remote-sensed solar radiation (which primarily detects clouds not smoke) as a predictor variable in place of air temperatures, but the resulting predictions poorly fit observed water temperatures. Estimates of the cooling effect of wildfire smoke on air temperature in the literature include observed 2-5 °C cooling of daytime air temps in 2010 in Colorado (Stone et al. 2011), modeled reductions of surface air temperatures in Alaska in 2004 by °2 C (Grell et al., 2011), difference between forecasted and observed daytime air temperatures of 1.5 to 7 °C in Canada during 1981 and 1982, Siberia in 1987, and Yellowstone National Park in 1988 (Robock, 1991), and daytime cooling of 5°C beneath a smoke plume over the Northeastern U.S. (Westphal and Toon, 1991). Dense smoke from fires in British Columbia resulted in temperatures in Washington D.C. being 2-6 °C cooler than forecast over a 4-day period in 1950 (Wexler, 1950). The most extreme example was in September 1987 at Happy Camp along the Klamath River when a persistent strong smoke inversion resulted in air temperatures 20 °C cooler than normal (Robock, 1988).

In our analysis, we use statistical regression models. An alternative approach would be deterministic models which simulate the underlying physics of heat flux between a stream and its environment (Caissie, 2006; Benyahya et al., 2007). Deterministic models are well suited to isolate the effect of a single parameter (i.e., smoke); however, such models are more time consuming to implement and require additional input parameters such as water depth and wind speed which are often unavailable. A new emerging method is a hybrid of the two which combines an equation based on physical principles with stochastic calibration of parameters and relies solely on air temperature and discharge as inputs (Piccolroaz et al. 2015; Toffolon and Piccolroaz, 2016), but unfortunately this would not allow us to quantify the effect of smoke.

Relative to air temperature and smoke, we found only a relatively weak correlation between water temperature and discharge (Figure 4, Table 1). In contrast, in a separate in-progress analysis of Salmon River temperature data (not shown here) which analyzes data at a monthly time scale rather than the daily time scale we use here, discharge explains nearly as much of the inter-annual variation in mean daily maximum August water temperature as air temperature does. These results indicate the benefits of analyzing data at multiple scales using multiple analytical approaches.

We found that the smoke effect on daily maximum temperatures was approximately twice the smoke effect on daily mean temperatures (Table 1). Daily means are influenced by both daily maxima and minima, so our result conform to previous studies that found that smoke affected daily maximum air temperatures much more than daily minimum temperatures (Robock, 1988; Robock, 1991; Stone et al., 2011). Maximum river water temperatures may be more important than mean temperatures as critical thresholds for chronic and acute stress for cold-water adaptive species (see Sullivan et al., 2000; Strange 2010).

We were able to successfully use a newly available MODIS MAIAC dataset of aerosol optical thickness to represent wildfire smoke. Other potential datasets for quantifying smoke include the standard 3 km or 10 km MODIS AOT products (Remer et al., 2013), new high-resolution algorithms for processing MODIS data such as SARA (Bilal et al., 2013, 2014) which has not yet been applied in North America, or aerosol products derived from other satellites such VIIRS (Visible Infrared Imaging Radiometer Suite) which launched in 2011 (Jackson et al., 2013), GOES Aerosol/Smoke Product (GASP) which has a 30-minute temporal resolution but low spatial resolution (12 x 12 km)(Prados, et al. 2007), or Advanced Very High Resolution Radiometer (AVHHR) which has a 40-year record which can be processed with an updated algorithm (Hsu et al., 2016). With the exception of the new Enterprise Processing System algorithm for VIIRS (Laszlo and Liu, 2016; Zhang et al., 2016) which will be available soon, all of these data sources have similar, or more severe, issues with clouds causing missing values as the MAIAC AOT.

In addition to using different AOT datasets, it would also be worth experimenting with alternative methods for filling gaps in the AOT data, such as by combining AOT with other datasets using more advanced methods such as geographically weighted regression (GWR; Gan et al., 2017; Lassman et al., 2017), geographically and temporally weighted regression (GTWR; Guo et al., 2017), regression kriging (Hengl, 2009; Sun et al., 2012; Meng, 2014), spatiotemporal regression-kriging (Hengl et al., 2012; Gräler et al. 2016), or inverse probability weights (IPW; Lee et al. 2016). Since smoke often occurs as inversions where smoke is more dense along canyon bottoms than ridgetops, local (i.e., moving window) regression kriging of AOT using elevation as the predictor variable might improve upon the spline interpolation method that we used, yet still be relatively simple to implement in R using either the rsaga and gstat packages. The gstat package can also perform spatio-temporal regression-kriging which could incorporate data from adjacent days (Gräler et al. 2016).

This analysis is a proof of concept to explore methods for analysis and provide an interim deliverable to fulfill contractual obligations. In an upcoming second phase of the project, we will refine our methods using alternative models and datasets, replicate the analysis at many additional sites within the Klamath Basin, and write a manuscript for submission to a peer-reviewed journal.

Acknowledgments

The Klamath Tribal Water Quality Consortium partially funded Riverbend Sciences' participation in this project. LeRoy Cyr (USFS) provided all Salmon River water temperature data. Qian Di (Harvard University) provided access to the MAIAC AOT data. James Szykman (NASA) and Todd Plessel (U.S. EPA) provided advice on remote sensed datasets. Nicolas Som (USFWS Arcata) provided statistical advice. The fisheries programs from the U.S. Forest Service (Six Rivers National Forest, Orleans Ranger District), Karuk Tribe, and Salmon River Restoration Council provided access and use of stream temperature data and local knowledge of wildfire, smoke, river water temperature, and fisheries observations. Susan Corum (Karuk Tribe), Crystal Robinson (Quartz Valley Indian Reservation), and Matt Hanington (Yurok Tribe) provided helpful comments on a draft of this report.

References

Abatzoglou J.T. (2013) Development of gridded surface meteorological data for ecological applications and modelling. *International Journal of Climatology*, **33**, 121–131.

Beakes M.P., Moore J.W., Hayes S.A. & Sogard S.M. (2014) Wildfire and the effects of shifting stream temperature on salmonids. *Ecosphere*, **5**, http://dx.doi.org/10.1890/ES13-00325.1

Behnke, R., S. Vavrus, A. Allstadt, T. Albright, W.E. Thogmartin, and V.C. Radeloff. 2016. Evaluation of Downscaled, Gridded Climate Data for the Conterminous United States. Ecological Applications 26:1338–1351. doi: 10.1002/15-1061.

Beitinger T.L. & Fitzpatrick L.C. (1979) Physiological and ecological correlates of preferred temperature in fish. *American Zoologist*, **19**, 319–329.

Benyahya L., Caissie D., St-Hilaire A., Ouarda T.B. & Bobée B. (2007) A review of statistical water temperature models. *Canadian Water Resources Journal*, **32**, 179–92.

Beschta R.L., Bilby R.E., Brown G.W., Holtby L.B. & Hofstra T.D. (1987) Stream temperature and aquatic habitat: fisheries and forestry interactions. In: Streamside management: forestry and fishery interactions. (Eds E.O. Salo & T.W. Cundy), pp. 191–232. Institute of Forest Resources, University of Washington, Seattle, Washington.

Bilal, M., J.E. Nichol, M.P. Bleiweiss, and D. Dubois, 2013. A Simplified High Resolution MODIS Aerosol Retrieval Algorithm (SARA) for Use over Mixed Surfaces. Remote Sensing of Environment 136:135–145. doi: 10.1016/j.rse.2013.04.014.

Bilal, M., J.E. Nichol, and P.W. Chan (2014) Validation and Accuracy Assessment of a Simplified Aerosol Retrieval Algorithm (SARA) over Beijing under Low and High Aerosol Loadings and Dust Storms. Remote Sensing of Environment 153:50–60. doi: 10.1016/j.rse.2014.07.015.

Bission, P.A.; Rieman, B.E.; Luce, C.; Hessburg, P.F.; Lee, D.C.; Kershner, J.L.; Reeves, G.H.; and Gresswell, R.E. (2003) Fire and aquatic ecosystems of the western USA: current knowledge and key questions. Forest Ecology and Management 178:213-229.

Brenning, A. (2008) Statistical geocomputing combining R and SAGA: The example of landslide susceptibility analysis with generalized additive models. In J. Boehner, T. Blaschke and L. Montanarella (eds.), SAGA - Seconds Out (= Hamburger Beitraege zur Physischen Geographie und Landschaftsoekologie, vol. 19), p. 23-32.

Caissie D. (2006) The thermal regime of rivers: a review. *Freshwater Biology*, **51**, 1389–1406.

California Air Resources Board (CARB). 2013. Almanac Emission Projection Data (published in 2013), 2012 Estimated Annual Average Emissions, Siskiyou County. California Environmental Protection Agency, Air Resources Board, Sacramento, CA. Online database: https://www.arb.ca.gov/app/emsinv/2013/emssumcat_query.php?F_YR=2012&F_DIV=0&F_SEASON=A&SP=2013&F_AREA=CO&F_CO=47

Chu, Y., Y. Liu, X. Li, Z. Liu, H. Lu, Y. Lu, Z. Mao, X. Chen, N. Li, M. Ren, F. Liu, L. Tian, Z. Zhu, and H. Xiang. 2016. A Review on Predicting Ground PM2.5 Concentration Using Satellite Aerosol Optical Depth. Atmosphere 7:129. doi: 10.3390/atmos7100129.

Daly, C., M. Halbleib, J.I. Smith, W.P. Gibson, M.K. Doggett, G.H. Taylor, J. Curtis, and P.P. Pasteris (2008). Physiographically Sensitive Mapping of Climatological Temperature and Precipitation across the Conterminous United States. International Journal of Climatology 28:2031-2064, DOI: 10.1002/joc.1688.

Di, Q., I. Kloog, P. Koutrakis, A. Lyapustin, Y. Wang, and J. Schwartz (2016) Assessing PM2.5 Exposures with High Spatiotemporal Resolution across the Continental United States. Environmental Science & Technology 50:4712–4721. doi: 10.1021/acs.est.5b06121.

Dunham J., Chandler G., Rieman B. & Martin D. (2005) Measuring stream temperature with digital data loggers: a user's guide. U.S. Department of Agriculture, Forest Service, Rocky Mountain Research Station. General Technical Report RMRSGTR- 150WWW.

Duncan, B.N., A.I. Prados, L.N. Lamsal, Y. Liu, D.G. Streets, P. Gupta, E. Hilsenrath, R.A. Kahn, J.E. Nielsen, A.J. Beyersdorf, S.P. Burton, A.M. Fiore, J. Fishman, D.K. Henze, C.A. Hostetler, N.A. Krotkov, P. Lee, M. Lin, S. Pawson, G. Pfister, K.E. Pickering, R.B. Pierce, Y. Yoshida, and L.D. Ziemba. 2014. Satellite Data of Atmospheric Pollution for U.S. Air Quality Applications: Examples of Applications, Summary of Data End-User Resources, Answers to FAQs, and Common Mistakes to Avoid. Atmospheric Environment 94:647–662. doi: 10.1016/j.atmosenv.2014.05.061.

Dunham J.B., Rosenberger A.E., Luce C.H. & Rieman B.E. (2007) Influences of wildfire and channel reorganization on spatial and temporal variation in stream temperature and the distribution of fish and amphibians. *Ecosystems*, **10**, 335–346.

Elder, D, B. Olson, A. Olson, and J. Villeponteaux (2002) Salmon River Sub-basin Restoration Strategy: Steps to Recovery and Conservation of Aquatic Resources: Report for The Klamath River Basin Fisheries Restoration Task Force, Interagency Agreement 14-16-0001-90532. USDA-Forest Service, Klamath National Forest, Yreka, Klamath National Forest and Salmon River Restoration Council, Sawyers Bar, CA. September 2002: 52 pp.

Estes, B.L., Knapp, E.E., Skinner, C.N., Miller, J.D. and Preisler, H.K., 2017. Factors influencing fire severity under moderate burning conditions in the Klamath Mountains, northern California, USA. Ecosphere, 8(5).

Gan, R.W., B. Ford, W. Lassman, G. Pfister, A. Vaidyanathan, E. Fischer, J. Volckens, J.R. Pierce, and S. Magzamen (2017) Comparison of Wildfire Smoke Estimation Methods and Associations with Cardiopulmonary-Related Hospital Admissions: Estimates of Smoke and Health Outcomes. GeoHealth 1:122–136. doi: 10.1002/2017GH000073.

Gergel, D.R., B. Nijssen, J.T. Abatzoglou, D.P. Lettenmaier, and M.R. Stumbaugh. 2017. Effects of Climate Change on Snowpack and Fire Potential in the Western USA. Climatic Change 141:287–299.

Gillooly J.F., Charnov E.L., West G.B., Savage V.M. & Brown J.H. (2002) Effects of size and temperature on developmental time. *Nature*, **417**, 70–73.

Gräler, B., E. Pebesma, and G. Heuvelink, 2016. Spatio-Temporal Interpolation Using Gstat. R Journal 8:204–218.

Grell, G., S.R. Freitas, M. Stuefer, and J. Fast (2011) Inclusion of Biomass Burning in WRF-Chem: Impact of Wildfires on Weather Forecasts. Atmospheric Chemistry and Physics **11**:5289–5303. doi: 10.5194/acp-11-5289-2011.

Gresswell R.E. (1999) Fire and aquatic ecosystems in forested biomes of North America. *Transactions of the American Fisheries Society*, **128**, 193–221.

Guo, Y., Q. Tang, D.-Y. Gong, and Z. Zhang (2017) Estimating Ground-Level PM2.5 Concentrations in Beijing Using a Satellite-Based Geographically and Temporally Weighted Regression Model. Remote Sensing of Environment 198:140–149. doi: 10.1016/j.rse.2017.06.001.

Hengl, T., 2009. A Practical Guide to Geostatistical Mapping of Environmental Variables. Office for Official Publications of the European Communities, Luxembourg. http://www.academia.edu/download/40396676/A_Practical_Guide_to_Geostatistical_Mapping.pdf

Hengl, T., G.B.M. Heuvelink, M.P. Tadic, and E.J. Pebesma (2012). Spatio-Temporal Prediction of Daily Temperatures Using Time-Series of MODIS LST Images. Theoretical and Applied Climatology 107:265–277. doi: 10.1007/s00704-011-0464-2.

Hitt N.P. (2003) Immediate effects of wildfire on stream temperature. *Journal of Freshwater Ecology*, **18**, 171–173.

Hsu, N.C., J. Lee, A.M. Sayer, N. Carletta, S.-H. Chen, C.J. Tucker, B.N. Holben, and S.-C. Tsay. 2017. Retrieving Near-Global Aerosol Loading over Land and Ocean from AVHRR. Journal of Geophysical Research: Atmospheres:2017JD026932. doi: 10.1002/2017JD026932.

Laszlo, I. and H. Liu, 2016. EPS Aerosol Optical Depth (AOD) Algorithm Theoretical Basis Document. https://www.star.nesdis.noaa.gov/jpss/documents/ATBD/EPS_ATBD_Aerosol_AOD_v3.0.1.pdf. Accessed 21 Aug 2017.

Isaak D.J., Luce C.H., Rieman B.E., Nagel D.E., Peterson E.E., Horan D.L., et al. (2009) Effects of climate change and recent wildfires on stream temperature and thermal habitat for two salmonids in a mountain river network. *Ecological Applications*, **20**, 1350–1371.

Jackson, J.M., H. Liu, I. Laszlo, S. Kondragunta, L.A. Remer, J. Huang, and H.-C. Huang, 2013. Suomi-NPP VIIRS Aerosol Algorithms and Data Products. Journal of Geophysical Research: Atmospheres 118:12,673-12,689. doi: 10.1002/2013JD020449.

Jankowski K., Schindler D.E. & Lisi P.J. (2014) Temperature sensitivity of community respiration rates in streams is associated with watershed geomorphic features. *Ecology*, **95**, 2707–2714.

Johnson, S.L. (2003) Stream temperature: scaling of observations and issues for modelling. Hydrol. Process. 17 (2), 497–499.

Johnson S.L. (2004) Factors influencing stream temperatures in small streams: substrate effects and a shading experiment. *Canadian Journal of Fisheries and Aquatic Sciences*, **61**, 913–923.

Lake F.K. (2007) Traditional ecological knowledge to develop and maintain fire regimes in Northwestern California, Klamath-Siskiyou bioregion: Management and restoration of culturally significant habitats. Dissertation, Oregon State University.

Lake F.K. (2009) Improving Our Understanding of Spatial and Temporal Effects of Wildfires on Forests, Riparian Zones, and Fisheries in the Klamath Mountains, United States of America. Presentation at Salmonid Restoration Conference, Santa Cruz, CA, March 7, 2009. US Forest Service-Pacific Southwest Research Station, Orleans, CA. http://srf.accelerantdesign.net/sites/default/files/2009%20SRF%20Procedings09_full_web.pdf

Lake F.K. (2013) Trails, fires, and tribulations: Tribal resource management and research issues in Northern California. *Occasion: Interdisciplinary Studies in the Humanities*, **5**, 1–22.

Lassman, W., B. Ford, R.W. Gan, G. Pfister, S. Magzamen, E.V. Fischer, and J.R. Pierce (2017) Spatial and Temporal Estimates of Population Exposure to Wildfire Smoke during the Washington State 2012 Wildfire Season Using Blended Model, Satellite, and in Situ Data. GeoHealth 1:2017GH000049. doi: 10.1002/2017GH000049.

Lee, M., I. Kloog, A. Chudnovsky, A. Lyapustin, Y. Wang, S. Melly, B. Coull, P. Koutrakis, and J. Schwartz (2016). Spatiotemporal Prediction of Fine Particulate Matter Using High-Resolution Satellite Images in the Southeastern US 2003–2011. Journal of Exposure Science and Environmental Epidemiology 26:377–384. doi: 10.1038/jes.2015.41.

Luce, C., B. Staab, M. Kramer, S. Wenger, D. Isaak, and C. McConnell (2014) Sensitivity of Summer Stream Temperatures to Climate Variability in the Pacific Northwest. Water Resources Research 50:3428–3443. doi: 10.1002/2013WR014329.

Lyapustin A., Martonchik J.V., Wang Y., Laszlo I., and Korkin S. (2011a) Multiangle implementation of atmospheric correction (MAIAC): 1. Radiative transfer basis and lookup tables. *Journal of Geophysical Research* **116**, D03210.

Lyapustin A., Wang Y., Laszlo I., Kahn R., Korkin S., Remer L., Levy R. & Reid J.S. (2011b) Multiangle implementation of atmospheric correction (MAIAC): 2. Aerosol algorithm. *Journal of Geophysical Research*, **116**, D03211.

Lyapustin A., Korkin S., Wang Y., Quayle B. & Laszlo I. (2012a). Discrimination of biomass burning smoke and clouds in MAIAC algorithm. *Atmospheric Chemistry and Physics*, **12**, 9679–9686.

Lyapustin A., Wang Y., Laszlo I. & Korkin S. (2012b) Improved cloud and snow screening in MAIAC aerosol retrievals using spectral and spatial analysis. *Atmosphere Measurement Techniques*, **5**, 843–850.

Mahlum S.K., Eby L.A., Young M.K., Clancy C.G. & Jakober M. (2011) Effects of wildfire on stream temperatures in the Bitterroot River Basin, Montana. *International Journal of Wildland Fire*, **20**, 240–247.

Mayer, T.D. (2012) Controls of Summer Stream Temperature in the Pacific Northwest. Journal of Hydrology 475:323–335. doi: 10.1016/j.jhydrol.2012.10.012.

Meng, Q. (2014) Regression Kriging versus Geographically Weighted Regression for Spatial Interpolation. International Journal of Advanced Remote Sensing and GIS 3:606–615.

Minshall G.W., Brock J.T. & Varley J.D. (1989) Wildfires and Yellowstone's stream ecosystems. BioScience, 39, 707–715.

Mitchell KE, Lohmann D, Houser PR, Wood EF, Schaake JC, Robock A, Cosgrove BA, Sheffield J, Duan Q, Luo L, Higgins RW, Pinker RT, Tarpley JD, Lettenmaier DP, Marshall CH, Entin JK, Pan M, Shi W, Koren V, Meng J, Ramsay BH, Bailey AA. (2004) The multi-institution North American Land Data Assimilation System (NLDAS): Utilizing multiple GCIP products and partners in a continental distributed hydrological modeling system. *Journal of Geophysical Research* 109: D07S90, DOI: 10.1029/2003JD003823.

Mohseni, O., H.G. Stefan, and T.R. Erickson, 1998. A Nonlinear Regression Model for Weekly Stream Temperatures. Water Resources Research 34:2685–2692. doi: 10.1029/98WR01877.

Neuheimer A.B. & Taggart C.T. (2007) The growing degree-day and fish size-at-age: the overlooked metric. *Canadian Journal of Fisheries and Aquatic Sciences*, **64**, 375–385.

North Coast Regional Water Quality Control Board (NCRWQCB). 2005. Salmon River, Siskiyou County, California Total Maximum Daily Load for Temperature and Implementation Plan Adopted June 22, 2005, NCRWQCB Resolution No. R1-2005-0058. Prepared by North Coast Regional Water Quality Control Board, Santa Rosa, California.

O'Laughlin, J. (2005) The Fire/Fish Risk Management Problem. Western Forester (March/April 2005): 12-13. http://www.forestry.org/sites/default/files/westernforester/2005/0405.pdf

Oyler, J.W., A. Ballantyne, K. Jencso, M. Sweet, and S.W. Running. (2014) Creating a Topoclimatic Daily Air Temperature Dataset for the Conterminous United States Using Homogenized Station Data and Remotely Sensed Land Skin Temperature. International Journal of Climatology 35:2258–2279. doi: 10.1002/joc.4127.

Piccolroaz, S., E. Calamita, B. Majone, A. Gallice, A. Siviglia, and M. Toffolon (2016) Prediction of River Water Temperature: A Comparison between a New Family of Hybrid

Models and Statistical Approaches. Hydrological Processes 30:3901–3917. doi: 10.1002/hyp.10913.

Pinheiro J., Bates D., DebRoy S., Sarkar D. & R Core Team. (2017) nlme: Linear and nonlinear mixed effects models. R package version 3.1-131.

Prados, A.I., S. Kondragunta, P. Ciren, and K.R. Knapp (2007) GOES Aerosol/Smoke Product (GASP) over North America: Comparisons to AERONET and MODIS Observations. Journal of Geophysical Research: Atmospheres 112:D15201. doi: 10.1029/2006JD007968.

R Core Team. (2015) R: A language and environment for statistical computing. R Foundation for Statistical Computing, Vienna, Austria.

Reid, C.E., M. Jerrett, M.L. Petersen, G.G. Pfister, P.E. Morefield, I.B. Tager, S.M. Raffuse, and J.R. Balmes. (2015) Spatiotemporal Prediction of Fine Particulate Matter During the 2008 Northern California Wildfires Using Machine Learning. Environmental Science & Technolog 49:3887–3896. doi: 10.1021/es505846r.

Rieman B.E., Gresswell R.E. & Rinne J.N. (2012) Fire and fish: A synthesis of observation and experience. In: Climate change, forests, fire, water, and fish: Building resilient landscapes, streams, and managers. (Eds C. Luce, P. Morgan, K. Dwire, D. Isaak, Z. Holden & B. Rieman), pp. 159–175. U.S. Department of Agriculture, Forest Service, Fort Collins, CO.

Remer, L.A., S. Mattoo, R.C. Levy, and L.A. Munchak (2013) MODIS 3 Km Aerosol Product: Algorithm and Global Perspective. Atmospheric Measurement Techniques 6:1829–1844. doi: 10.5194/amt-6-1829-2013.

Robock A. (1988) Enhancement of surface cooling due to forest fire smoke. *Science*, **242**, 911–913.

Robock A. (1991) Surface cooling due to forest fire smoke. *Journal of Geophysical Research*, ***96***, 20869–20878.

Robinson, C. 2013. 2013 Water Quality Study Including Impacts from Fire Salmon River, CA. Karuk Department of Natural Resources, Somes Bar, CA.

Robinson, C. 2014. 2013 Salmon River Water Quality and Fire Impacts. Presentation to the Klamath Basin Monitoring Program meeting, Yreka in CA on April 17, 2014. Karuk Tribe Department of Natural Resources, Somes Bar, CA. http://www.kbmp.net/images/stories/pdf/KBMP_minutes/meeting_14/10.%202013%20Salmon%20River%20Water%20Quality%20and%20Fire%20Impacts_Karuk%20Tribe.pdf

Salmon River Restoration Council (SRRC). 2014. Parched Rivers Smoking Skies: a Year of Drought and Fire on the Salmon River. Salmon River Restoration Council, Sawyers Bar, CA. 14p. http://www.srrc.org/publications/newsletters/SRRC%20Fall-Winter%202014%20Newsletter.pdf

Short K.C. (2014) A spatial database of wildfires in the United States, 1992-2011. Earth System Science Data, 6, 1–27.

Short K.C. (2015) Spatial wildfire occurrence data for the United States, 1992-2013 [FPA_FOD_20150323]. 3rd Edition. Forest Service Research Data Archive. https://doi.org/10.2737/RDS-2013-0009.3

Smith, H.G., G.J. Sheridan, P.N.J. Lane, P. Nyman, and S. Haydon, 2011. Wildfire Effects on Water Quality in Forest Catchments: A Review with Implications for Water Supply. Journal of Hydrology 396:170–192. doi: 10.1016/j.jhydrol.2010.10.043.

Stone R.S., Augustine J.A., Dutton E.G., O'Neill N.T. & Saha A. (2011) Empirical determinations of the longwave and shortwave radiative forcing efficiencies of wildfire smoke. *Journal of Geophysical Research: Atmospheres*, **116**, D12207.

Sun, W., B. Minasny, and A. McBratney, 2012. Analysis and Prediction of Soil Properties Using Local Regression-Kriging. Geoderma 171:16–23. doi: 10.1016/j.geoderma.2011.02.010.

Superczynski, S.D., S. Kondragunta, and A.I. Lyapustin, 2017. Evaluation of the Multi-Angle Implementation of Atmospheric Correction (MAIAC) Aerosol Algorithm through Intercomparison with VIIRS Aerosol Products and AERONET: MAIAC AOT Evaluation. Journal of Geophysical Research: Atmospheres 122:3005–3022. doi: 10.1002/2016JD025720.

Toffolon, M. and S. Piccolroaz (2015) A Hybrid Model for River Water Temperature as a Function of Air Temperature and Discharge. Environmental Research Letters 10:114011. doi: 10.1088/1748-9326/10/11/114011.

Taylor A.H. & Skinner C.N. (1998) Fire history and landscape dynamics in a late-successional reserve, Klamath Mountains, California, USA. *Forest Ecology and Management*, **111**, 285–301.

Taylor A.H. & Skinner C.N. (2003) Spatial patterns and controls on historical fire regimes and forest structure in the Klamath Mountains. *Ecological Applications*, **13**, 704–719.

Turco, R.P., O.B. Toon, T.P. Ackerman, J.B. Pollack, and C. Sagan, 1990. Climate and Smoke: An Appraisal of Nuclear Winter. Science 247:166–176. doi: 10.2307/2873486.

Webb, B.W., D.M. Hannah, R.D. Moore, L.E. Brown, and F. Nobilis (2008). Recent Advances in Stream and River Temperature Research. Hydrological Processes 22:902–918.

Webb B.W., Clark P.D. & Walling D.E. (2003) Water-air temperature relationships in a Devon river system and the role of flow. *Hydrological processes*, **17**, 3069–3084.

Westerling, A.L. and B.P. Bryant (2008) Climate change and Wildfire in California. Climatic Change 87 (Suppl 1): S231-S249.

Westerling, A.L., B.P. Bryant, H.K. Preisler, T.P. Holmes, H.G. Hidalgo, T. Das, and S.R. Shrestha (2011) Climate change and growth scenarios for California wildfire. Climatic Change 109 (Supp 1): S445-S463. DOI 10.1007/s10584-011-0329-9

Wexler, H., 1950. The Great Smoke Pall — September 24–30, 1950. Weatherwise 3:129–142. doi: 10.1080/00431672.1950.9927067.

Wiedinmyer C., Akagi S.K., Yokelson R.J., Emmons L.K., Al-Saadi J.A., Orlando J.J. & Soja A.J. (2011) The Fire Inventory from NCAR (FINN): a high resolution global model to estimate the emissions from open burning. *Geoscientific Model Development*, **4**, 625–641.

Yu, P., O.B. Toon, C.G. Bardeen, A. Bucholtz, K.H. Rosenlof, P.E. Saide, A. Da Silva, L.D. Ziemba, K.L. Thornhill, J.-L. Jimenez, P. Campuzano-Jost, J.P. Schwarz, A.E. Perring, K.D. Froyd, N.L. Wagner, M.J. Mills, and J.S. Reid, 2016. Surface Dimming by the 2013 Rim Fire Simulated by a Sectional Aerosol Model: Rim Fire Simulation. Journal of Geophysical Research: Atmospheres 121:7079–7087. doi: 10.1002/2015JD024702.

Zhang, H., S. Kondragunta, I. Laszlo, H. Liu, L.A. Remer, J. Huang, S. Superczynski, and P. Ciren, 2016. An Enhanced VIIRS Aerosol Optical Thickness (AOT) Retrieval Algorithm over Land Using a Global Surface Reflectance Ratio Database. Journal of Geophysical Research: Atmospheres 121:2016JD024859. doi: 10.1002/2016JD024859.